# *Ab initio* interface configuration determination for β'' in Al–Mg–Si: beyond the constraint of a preserved precipitate stoichiometry

Flemming J. H. Ehlers*

Dept. of Physics, Norwegian University of Science and Technology (NTNU), 7491 Trondheim, Norway

* Corresponding Author: Flemming J. H. Ehlers

Dept. of Physics, Norwegian University for Science and Technology NTNU, 7491 Trondheim, Norway

email: flemming.ehlers@ntnu.no

Tel: +47 7359 3480; Fax: +47 7359 7710

## Abstract

The precipitate-host lattice interface configuration stabilities for the β" phase in the Al–Mg–Si alloy system have been examined using density functional theory. Usually, the supercell based calculations underlying such studies assume a preserved precipitate stoichiometry. Relaxing this assumption in the present work, we highlight significant results that may easily be overlooked when the stoichiometry constraint is operative. Our main findings are the following: (i) we reject the often proposed $Mg_5Si_6$ composition for β". (ii) We stress the possibility of significant Mg–Al compositional disorder for the more likely β"–$Mg_5Al_2Si_4$. Finally, (iii) we propose the existence of more than one locally stable interface configuration for the coherent β"/Al interfaces. It is argued that quantifying the solute atom diffusivity near the interface as well as within β" is fundamental to addressing the importance of points (ii) and (iii).

**Keywords:** First-principles calculations, Aluminium alloys, Precipitate-host lattice interfaces,

Interface configuration stabilities, Metastable phase compositional disorder

## 1. Introduction

Age hardenable Al–Mg–Si(–Cu) alloys are of considerable interest to industry for both engineering, marine, and transport applications. Among the desirable properties of these materials are their high strength/weight ratio, good formability and weldability, and excellent corrosion resistance. Upon the 'ageing' heat treatment following forming, a significant hardness increase can be achieved. This is attributed to the emergence of a high density of metastable (semi-)coherent precipitates that form obstacles to the dislocation flow in the face-centred cubic (fcc) Al host lattice. The close link of atomic-level mechanisms with macroscopic behaviour has triggered a wealth of experimental studies over the last decade (see, e.g., [1 – 4]). It is generally acknowledged that full optimization of materials properties requires that precipitate structures and compositions be clarified, including correlations between number densities and heat treatment. For the Al–Mg–Si alloy, the main hardening phase is the fully coherent needle-shaped β" [5, 6]. The structure of this precipitate was clarified originally by Zandbergen et al. [7, 8], though some debate remains as to the β" composition [9, 3]. It is conceivable that β", being the first accepted post–Guinier Preston (GP) zone [10] to appear in Al–Mg–Si upon ageing [11], hosts appreciable levels of compositional disorder.

Complementing the experimental studies, multi-scale modelling schemes show an increasing ability to connect atomistic and macroscopic length scale properties theoretically (see, e.g., [12 – 14]). Consequently, there is a growing desire [15] to use calculations as a cheap and fast guideline to experimental investigations for the alloy optimization procedure. In this context, the importance of reliable atomic-level approximations to the precipitate-host lattice interfacial energies is well established [16]. Contrasting this desire for accuracy, however, practical density functional theory

(DFT) based studies of the β"/Al interfaces [17, 18] have so far involved decisively crude approximations. The chosen set of interface configurations for the supercells underlying these studies are conventionally subjected to the constraint of a *preserved precipitate stoichiometry*, equal to the presumed bulk phase composition. Technically, such a constraint is necessary in order that the interfacial energy be accurately identified [17]. Physically, however, there is no sound reasoning behind neglecting precipitate composition variations near the interface, or constraining the interface configurations with reference to a bulk phase property. Recent experimental studies [19, 20] stress examples of clear deviations from this path. Further, the theoretical approach to identifying the lowest interface energy configuration in the presence of the above described 'stoichiometry constraint' is dubious. Typically, the supercells allowed by this constraint will host pairs of inequivalent configurations, preventing clarity on the issue of relative *single* configuration stabilities. Indeed, mixing competing configurations in this analysis may be a dominant source of errors to zero temperature investigations. This would simply reflect the relative importance of interface chemical interactions over misfit strain. A more complete procedure for identifying the stable interface configuration(s) would appear desirable.

In this work, we relax the stoichiometry constraint in studies of the known coherent interfaces of the β" phase with Al. Retaining the assumption [17] of compositionally abrupt interfaces for this system, we discuss how the interface evolution may be strongly affected by local growth obstacles according to our studies. These previously unnoticed features may trigger appreciable phase compositional disorder while also locally stabilizing more than one interface configuration. We stress that these proposed modifications may still be compatible with the most recently reported β" composition [9].

This paper is managed as follows: in Sec. 2, we firstly present the system under investigation.

Subsequently, we outline our basic assumptions for the precipitate growth, stressing the deviations from earlier studies. Finally, our suggested procedure for identifying a stable interface configuration candidate within a supercell based scheme is described. Sec. 3 discusses computational details, while Sec. 4 presents the main results of this work. In Sec. 4.1, we describe the results of bulk β" phase optimization, highlighting the importance of Mg-rich configurations previously ignored in the literature. Sec. 4.2, 4.3 discuss the two β"/Al interfaces where experimental information is available: the $(130)_{Al}$ and the $(–320)_{Al}$ interface, respectively. In Sec. 5, we discuss the results obtained, while a summary of our main findings is provided in Sec. 6. In Appendix A, B, the convergence of our results with respect to key input parameters (cell size and precision) has been examined.

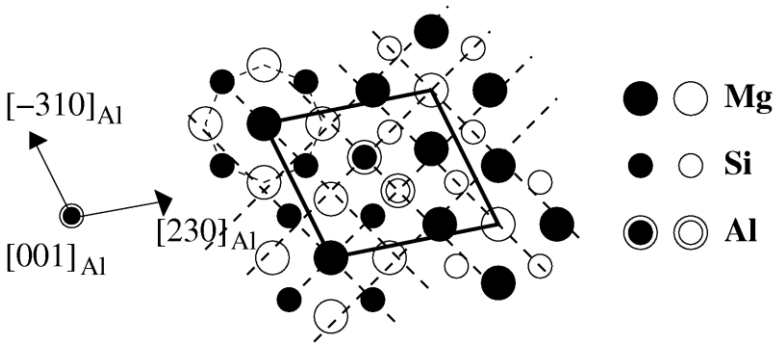


**Fig. 1.** Schematic illustration of the primitive unit cell for the monoclinic β" structure ($Mg_5Al_2Si_4$ composition chosen). The unit cell is delimited by full broad lines. Only two atom heights (difference 2.025 Å) are adopted along $[001]_{Al}$. The broad dashed lines stress the close connection of β" to the fcc Al host lattice: the atoms of the latter phase occupy sites located at the intersection of the lines (precipitate expansion relative to host ignored), with only the height of the β" 'eye' atom at the cell corner changed from black to white or vice versa. A β" 'eye unit', surrounding this eye atom, has been highlighted with thin dotted lines in the upper left corner of the unit cell.

## 2. Methodology and previous work

*2.1. The bulk β″ precipitate*

A schematic presentation of the monoclinic β" structure (space group C2/m) is shown in Fig. 1 [21]. Here, the close structural connection between β" and the fcc Al host lattice is highlighted. Only one atom per β" unit cell, located at the cell corner, adopts a markedly different position – an octahedral interstitial (I) site in the host. This atom is often labelled the 'eye' atom, due to the appearance of the surrounding geometry in transmission electron microscopy (TEM) images. The full geometry will be named an 'eye unit' below. This is motivated by the apparent coincidence of the observed β"/Al structural interfaces [8] with the compositional interfaces obtained when insisting that β" be comprised by a whole number of such atom configurations.

The observed β"/Al orientation relationships [5], indicated in Fig. 1 as well for clarity, read:

$$[230]_{Al} \parallel [100]_{\beta''}^{Conv.}; [001]_{Al} \parallel [010]_{\beta''}^{Conv.}; [-310]_{Al} \parallel [001]_{\beta''}^{Conv.}. \quad (1)$$

These relationships can be understood directly from the information provided in the figure, when taking into account the connection of the β" conventional and primitive unit cells: $\mathbf{a}_{\beta''}^{Conv.} = 2\mathbf{a}_{\beta''}^{Prim.} - \mathbf{b}_{\beta''}^{Conv.}$. As discussed in, e.g., [8], the experimentally observed β"/Al interfaces are coherent and located in the planes spanned by the precipitate basis vectors. This subset comprises the $(130)_{Al}$ and $(-320)_{Al}$ interfaces, hence also frequently referred to as the **cb** and **ab** interfaces, respectively, below. The associated interface configurations are discussed in Sec. 2.2.2. The **a** and **c** basis vectors define directions of appreciable precipitate-host lattice misfits [8], while the subsystem misfit along **b** (the β" needle direction) is rendered negligible. For the needle ends, no TEM based information on the nature of the interface is achievable.

Originally, an $Mg_5Si_6$ composition was proposed for β" from experimental studies [7]. More

recently, it was concluded from atom probe tomography (APT) experiments [9] that β" is likely to host ≈ 20% Al, with these atoms primarily replacing Si. DFT calculations in the same work highlighted 'significant energy penalties' for Al introduction on all Si sites but those ultimately fully occupied by Al in Fig. 1. It follows that the resulting Si substructure (the 'Si network' [9]) in the proposed β"–$Mg_5Al_2Si_4$ phase is likely very resistant to compositional disorder. Other extensive APT studies [22, 3] have supported a β" Mg/Si ratio close to 1.1, seemingly favouring the $Mg_5Al_2Si_4$ over the $Mg_5Si_6$ composition [23]. The level of β" compositional disorder – beyond the Si network in particular – remains a matter of debate, however. This is partly due to the close links of current results to APT, combined with the limits on spatial resolution for this technique. Further, the theoretical studies of [9] neglected deviations from C2/m symmetry for the β" unit cell and assumed an upper limit of 45% Mg in the precipitate. These simplifications may well exclude configurations important to revealing β" compositional disorder. For this reason, we have carried out a more complete theoretical examination of the β" configuration stabilities in the present work, with the results included in Sec. 4.1.

### *2.2. Basic considerations on β" growth*

#### *2.2.1. The level of atom diffusion within β"*

Clarifying the level of compositional disorder in β" (see Sec. 2.1) must ultimately be closely connected with quantifying the level of diffusion in the precipitate. Normally, no constraints on this parameter are imposed in theoretical considerations, see, e.g., [11]. When examining the available experimental data on this issue, the case however seems less clear-cut. Below, we outline the main aspects of these considerations.

Upon ageing, β" is ultimately replaced by other, structurally and compositionally clearly distinct metastable phases [1, 24, 25]. Hence, if β" should transform to a post-β" phase by aid of internal

structural transformation, a high level of solute atom diffusion within the precipitate would necessarily be implied. To our knowledge, however, no direct experimental observation of such modes of transition is found in the literature. Also the average composition variation over the course of evolution of a *given* β" precipitate is presently shrouded in uncertainty. Arguably the best method available for probing this issue, APT experiments [22] do suggest a gradually changing microstructure composition towards peak hardness. However, the analysis of this feature is complicated by a series of points: (i) the microstructure evolution over this range typically involves a transition from the GP zone pre–β" to β" [6]. (ii) Like β", pre–β" has a needle morphology, but possibly adopts a different, more Mg-Si balanced composition [22, 26]. Finally, (iii) the microstructure is undergoing significant coarsening during the pre–β" → β" transformation [6]. It follows that the distinction of these two phases, and hence the mode of structural transition, may be elusive in APT.

Composition variations over time for the β" phase have also been proposed [11] on the basis of TEM studies. More recently, however, the main conclusions of that work have been put strongly in doubt. It was shown in [9] that the 'Si nanopillars', hypothesized as integral to β"–$Mg_5Si_6$ formation in [11], can be strongly altered without energy penalty. With the existence of such nanopillars proposed directly from experimental observation in [11], it must seem unclear how well the different atom types Al, Mg, and Si can actually be distinguished with TEM.

Based on the above considerations, we conclude the following: an interface model scheme (Fig. 2a) confining both the structural and compositional evolution of β" to the interface region – by assuming low diffusivity elsewhere in the precipitate – is not necessarily to be viewed as artificially constrained. Rather, such a scheme should be judged from a comparison of its predictions with experiment. These thoughts describe the approach followed in the present work.

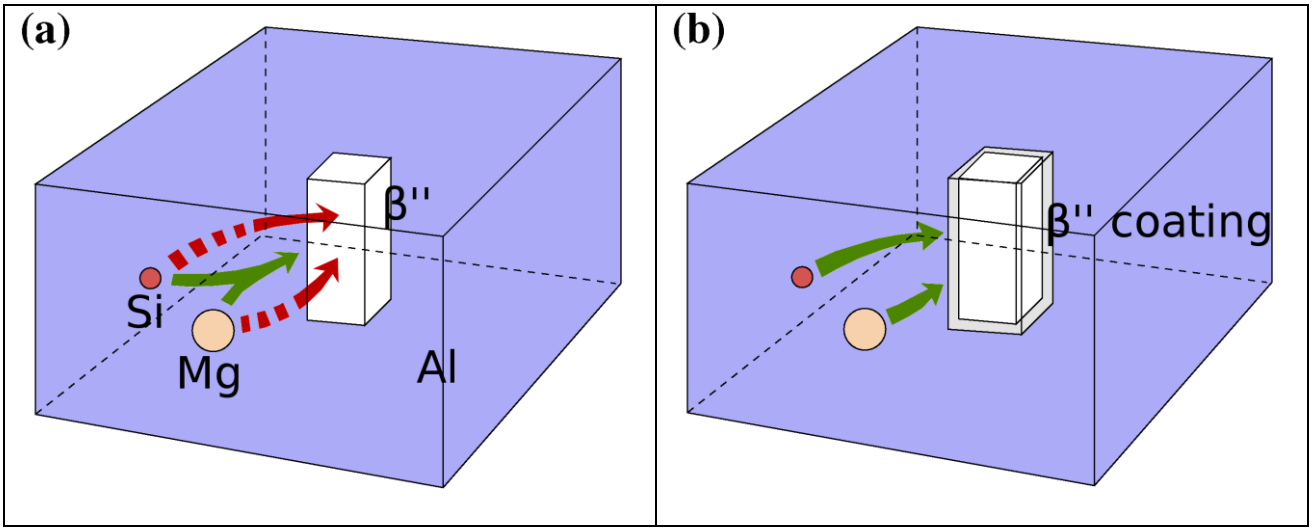


**Fig. 2.** Schematic illustrations of the dominant modes of growth of β" in fcc Al assumed operative in this work. The selected solute atoms are not drawn to scale. (a) Diffusion into the precipitate during growth (red dashed arrows) is presumed negligible, implying that the precipitate evolves essentially in the interface region (full green arrow). Here, (b) it is conceivable that both a different structure (most likely pre–β") and composition is adopted, explaining the precipitate 'coating' shown.

*2.2.2. The β"/Al interfaces*

As mentioned in Sec. 2.2.1, the evolution of β" appears closely coupled to its precursor phase pre–β". Despite being typically categorized as a GP zone in the literature, pre–β" has also been viewed [26, 27] as adopting a structure with space group C2/m. In this picture, differences to β" are confined to the eye atom position, phase composition and level of compositional disorder. Following the definition of a GP zone [10], the β" eye atom must be relocated in pre–β", on the nearest substitutional (S) site for the underlying host lattice (see Fig. 1).

The pre–β" → β" structural transition has been discussed theoretically in earlier work [11, 27]. In both cases, gradual composition changes throughout the precipitate were assumed. As discussed in

Sec. 2.2.1, we view this assumption as presently hypothetical. In the vicinity of the β"/Al interface, however, both the phase composition and structure may well be altered in general. Support for this hypothesis is obtained from experimental high angle annular dark field scanning TEM (HAADF-STEM) studies of other precipitates observed in Al–Mg–Si and closely related alloy systems [28, 20]. Here, a 'coating' of a bulk precipitate phase (β') with a similar, but more coherent structure was reported. For β", a pre–β" coating (see Fig. 2b) would likewise appear probable, judged from the close structural connection of pre–β" and fcc Al. Further, the lower β" growth temperature may represent an obstacle to eye atom movements near the interface, depending on local composition [27]. This may again promote pre–β" formation at the interface.

To our knowledge, no rigorous analysis of β"/Al interfaces with HAADF-STEM has been published. Hence, for reasons discussed in Sec. 2.2.1, the issue of interface configuration stabilities must be regarded as still being in its infancy. Structurally (see Sec. 2.1), β" typically appears to be comprised by a whole number of eye units. The coinciding compositional interface is labelled the structural interface (SI) configuration here. Originally, Andersen et al. [8] proposed a more Si-rich configuration for the **ab** interface. More recently, calculations by Wang et al. [17] supported an SI configuration stability for both the **ab** and **cb** interfaces. This theoretical study however was hampered by the stoichiometry constraint discussed in Sec. 1. We do not limit our investigations by any of this earlier work.

*2.3. Identifying stable β"/Al interface configurations*

As discussed in Sec. 2.2, we are assuming in the present work that precipitate composition modifications are confined to the interface vicinity. Experimentally, there is evident support – through the observed rhomboid precipitate cross-section shape – for at least one highly stable interface configuration. It follows that, in our model scheme, β" must necessarily evolve by near

layer-by-layer growth. Depending on the level of diffusion constraints near the interface, the focus of the interface configuration stability investigation may in turn be shifted from identification of global [17] to *local* interface energy minima. In the case of low diffusion everywhere in β", each significant obstacle on the growth path should be of importance as highlighting a long-lived configuration. These considerations form the basis of the strategy presented below.

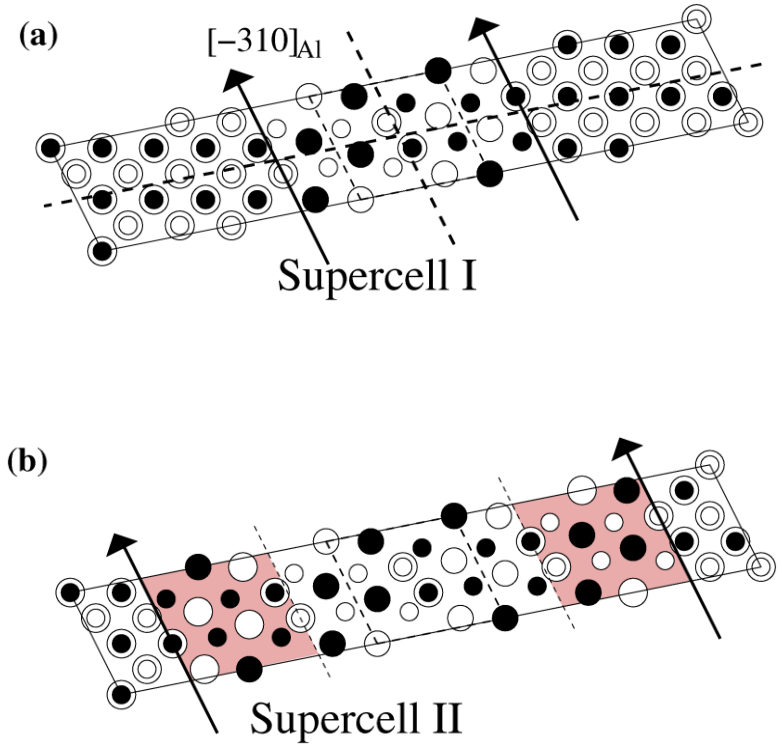


**Fig. 3.** Schematic presentation of two β"/Al supercells describing the same $(130)_{Al}$ or **cb** interface configuration. For the choice of atom labelling, see Fig. 1. (a) Supercell I: precipitate (subsystem between the arrows) containing 22 atoms, with the Al atoms divided by the arrows viewed as belonging to β". A β" primitive unit cell has been highlighted with thin dashed lines, while also, lines running through the precipitate inversion symmetry point have been shown. (b) Supercell II: precipitate containing 44 atoms (22 host lattice atoms replaced, compared to (a)). The shaded regions, showing the β" extension relative to (a), is equivalent to two β" primitive unit cells. Subsystem volume differences have been ignored throughout.

Consider a β"–$Mg_5Al_2Si_4$/Al **cb** interface region supercell, referred to here as 'I' (see Fig. 3a), as constructed (see also Sec. 3.2) employing the precipitate-host lattice orientation relationships (1). The interface configurations at either side of the precipitate are presumed identical, and compositionally sharp. The precipitate part of the supercell is now extended at each interface, at the expense of the host lattice part, to the point ('II', see Fig. 3b) where the *same* interface configuration is reached once again. Since the precipitate evolution thus described is periodic, it follows that all compositionally sharp and closely planar β"/Al interface configurations can be viewed as being present somewhere on a growth path between supercells I and II.

To see how the two cells of Fig. 3 may form a useful basis for investigations into the individual interface configuration stabilities, consider the associated system energies. It is generally acknowledged that the bulk formation enthalpy $\Delta H_{\mathrm{P,\,Bulk}}$ of a precipitate 'P', as determined relative to isolated solute atoms in the host, vastly exceeds the interface energy. Hence, the full formation enthalpy change upon extending the β" precipitate as described in Fig. 3 should be well approximated by neglecting subsystem interaction effects:

$$N_{\mathrm{II}}\Delta H_{\mathrm{II,\,Full}} \approx N_{\mathrm{I}}\Delta H_{\mathrm{I,\,Full}} + N_{\beta''}\Delta H_{\beta'',\,\mathrm{Bulk}}. \qquad (2)$$

Here, the subscript I (II) refers to the cell shown in Fig. 3a (b). The quantities $N_{\mathrm{I}}$, $N_{\mathrm{II}}$ and $N_{\beta''}$ describe the number of solute atoms contained in cells I, II, and the β" conventional unit cell, respectively.

Consider now a chosen β" growth path, involving a full sequence of logically connected cells $\{i\}$ linking I and II. Returning to the comments at the beginning of this section, any candidate $i$ for a

stable interface configuration on this path should be associated with a local interface energy minimum. Such a minimum can be highlighted straightforwardly when subtracting from the system enthalpy difference $H_i - H_\mathrm{I}$ two quantities: (i) the formation enthalpies for the atoms exchanged with regions elsewhere in the host lattice in the process of obtaining $i$ from I. (ii) The full formation enthalpy change for the precipitate in cell $i$ relative to I, as estimated with (2). With the resulting energy labelled $\Delta H_i$,

$$\begin{aligned}\Delta H_i \quad &= (H_i - H_\mathrm{I}) - (N_{i,\,\mathrm{Mg+Si}} - N_{\mathrm{I},\,\mathrm{Mg+Si}})\Delta H_\mathrm{Al}^\mathrm{SS} - (N_{i,\,\mathrm{Si}} - N_{\mathrm{I},\,\mathrm{Si}})\Delta H_\mathrm{Si}^\mathrm{SS} \\ &\quad - (N_{i,\,\mathrm{Mg}} - N_{\mathrm{I},\,\mathrm{Mg}})\Delta H_\mathrm{Mg}^\mathrm{SS} - (N_i - N_\mathrm{I})\Delta H_{\beta'',\,\mathrm{Bulk}}. \qquad (3)\end{aligned}$$

Here, the parameter $N_{i,\,\mathrm{X}}$ denotes the number of solute atoms of type X in the precipitate of cell $i$, with the remaining parameters in parentheses having the logical interpretation derived from the comments following (2). The label ‘SS’ stresses how the calculated formation enthalpies for solute atoms X should mimic the quenched-in supersaturated solid solution at the earliest stages of precipitate formation in the Al–Mg–Si alloy system. The last term on the RHS of (3) is featureless by construction, implicitly assuming the *same* binding energy of each new atom added to the precipitate [29]. By contrast, the growth path under investigation, described through the remaining terms on the RHS of (3), incorporates the interface energies from direct calculation on the cells making up the path $\{i\}$. A schematic presentation of the potential outcome of (3), highlighting the values $\Delta H_i$ for each configuration from the set $\{i\}$, is shown in Fig. 4.

The example provided above tells us that a configuration (cell $i$) that represents a 'sufficiently deep' local energy minimum in Fig. 4 is to be regarded as stable for the selected growth path comprised by the set of configurations $\{i\}$. For the interface configuration to satisfy the fundamental requirements of true local stability, this minimum energy property should apply to *all* growth paths

passing through this cell. In such a case, any last (next) added atom to this configuration would possess a binding energy significantly stronger (weaker) than the average value. An even stronger statement emerges if the growth path passing through cell *i* appears the most physically sound choice – i.e., connected with the lowest level of obstacles to the evolution from cell I to II. In such a case, the interface configuration connected with cell *i* must appear a *necessity*, and hence a candidate for a stable, experimentally observable configuration. We note that, to the extent that (3) is well obeyed, this expression represents a simple generalization of the concepts used for evaluating interface configuration stabilities in, e.g., [17].

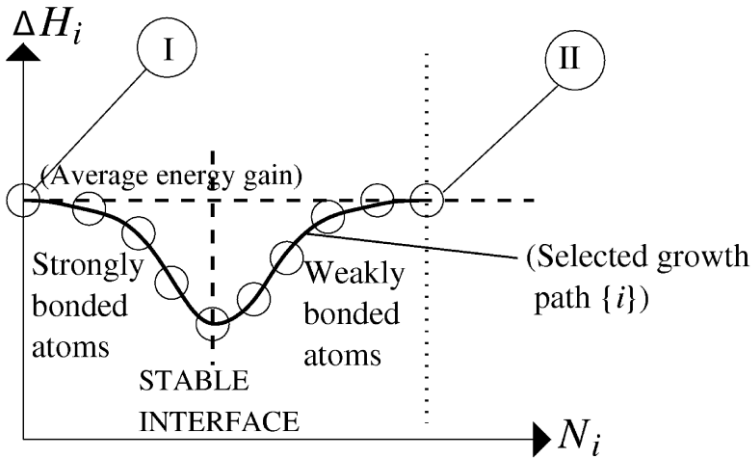


**Fig. 4.** Comparison of the average precipitate formation enthalpy gain when moving from supercell I to II in Fig. 3 (i.e., extending β" by a whole cycle of interface configurations) with proposed more realistic contours of the enthalpy variation with precipitate size, using the expression (3). See text for details.

## 3. Computational details

### *3.1. Energies and units*

The computational studies of this work has two main aims: as discussed in Sec. 2.1, we wish to examine more closely the bulk β" configurations, in addition to the interface configuration

studies described in Sec. 2.3. For the former investigation, the precipitate bulk formation enthalpy $\Delta H_{\beta'', \mathrm{Bulk}}$, as obtained relative to isolated solute atoms in fcc Al, is computed for a representative set of β" configurations. This strategy follows the work of Hasting et al. in [9], though our choice of precision (see Sec. 3.3) is different. The bulk formation enthalpy of a general β"–$Mg_xAl_{7-x-y}Si_{4+y}$ configuration (see Sec. 4.1 for details) is defined as:

$$\Delta H_{\beta'', \mathrm{Bulk}} = H(\beta''\text{–}Mg_xAl_{7-x-y}Si_{4+y}) - x\Delta H_{Mg}^{SS} - (7-x-y)\Delta H_{Al}^{SS} - (4+y)\Delta H_{Si}^{SS}; \quad (4)$$

$$\Delta H_X^{SS} = H(\mathrm{fcc}\text{–}Al_{107}X) - (107/108)H(\mathrm{fcc}\text{–}Al_{108}). \quad (5)$$

In these expressions, *H* denotes enthalpies for the respective systems described in parenthesis. The formally isolated solute atoms 'X' in (5) approximate the quenched-in SS, as discussed in Sec. 2.3. In practice, we ignore finite temperatures, zero temperature vibrational contributions, and non-zero pressure contributions in our studies. The remaining discussions in this text are modified accordingly, making reference to *formation energies*, e.g., $\Delta E_{\beta'', \mathrm{Bulk}}$. For comments on this choice of strategy, also applied to the interface studies, see Sec. 5.

We shall operate with two sets of units throughout the work. The bulk β" formation energies are obtained in units of eV/solute atom. For comparison with these values, interface configuration local stabilities are examined in the same manner, i.e., binding energies for solute atoms added to a given configuration are presented in these units as well. On the other hand, interface energies are conventionally described in units of kJ/mole atom. For the studies connected with (3), we therefore use this unit for easier comparison with the literature. All interface supercells examined contain pairs of equivalent interface configurations. In this scenario, the supercell precipitate always possesses inversion symmetry around its centre (see, e.g., Fig. 3a). Hence, to probe relative single

interface configuration stabilities, the output energies from (3) were ultimately divided by a factor two.

*3.2. Interface supercell construction*

In all β"/Al supercell calculations described in Sec. 4, cells containing 55 atoms (examples shown in e.g. Fig. 3 for the $(130)_{Al}$ interface) were used. The construction of these cells employed fcc Al supercells, obtained using the one-to-one correspondence of precipitate and host lattice sites outlined in Fig. 1. Earlier theoretical studies [17] have indicated that a 44 atom cell with 22 atoms in the precipitate is sufficiently large for computation of the interfacial energies. In the present work (see Fig. 3, 4), we want to examine a *range* of interface configurations, however, with the associated precipitate size variation covering 22 atoms. For such studies, a 55 atom cell would appear a minimum requirement for acceptable accuracy. Ultimately, convergence of the main results of Sec. 4 with respect to cell size was tested (see Appendix A), with the conclusion that the 55 atom cells are sufficiently large.

*3.3. Precision in the studies*

The zero temperature total energy calculations were performed within the framework of DFT [30, 31], using Vanderbilt ultrasoft pseudopotentials [32] as implemented in the plane wave (PW) based Vienna *ab initio* Simulation Package (VASP) [33, 34]. The Perdew-Wang generalized gradient correction (GGA) to the exchange-correlation functional [35] was employed throughout. Based on earlier studies [18], we chose a PW cut-off of 225 eV in the simulations, and (2, 22, 14), (12, 22, 3) Monkhorst-Pack *k*-point grids for the β"/Al **cb** and **ab** supercells, respectively. A corresponding precision was used in the studies of bulk β" and fcc Al. In all calculations, full relaxation (optimization of cell dimensions and basis vector angles, in addition to cell atom positions) was performed. As discussed in Appendix B, this level of precision was found to be

sufficiently high for relative configuration energies to be converged within a few hundredths of a kJ/mole atom – well below any of the energy differences discussed throughout this work.

## 4. Results

### *4.1. The bulk β" structure*

In the present work, we relax the two constraints (see Sec. 2.1) on bulk β" configuration optimization of earlier work [9], optimizing all bulk β"–$Mg_xAl_{7-x-y}Si_{4+y}$ configurations with $x \geq 4$, $y \geq 0$. Following preliminary discussions, we still require 100% Si atoms on the (four) network sites throughout. The chosen set hosts both the β"–$Mg_5Al_2Si_4$ configuration proposed on the basis of the APT studies by Hasting et al. [9] as well as the original candidate β"–$Mg_5Si_6$ reported in [7].

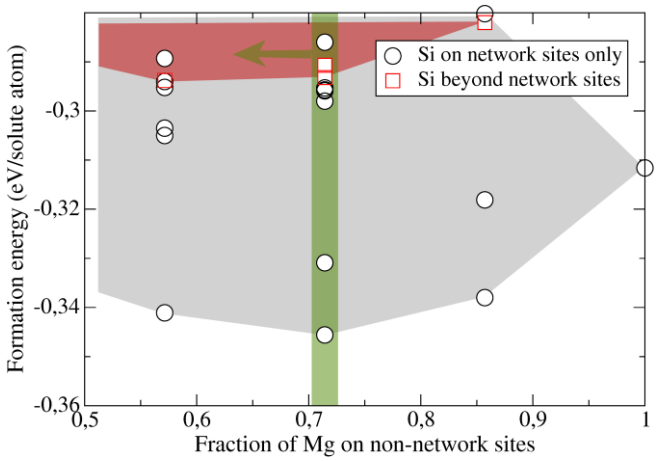


**Fig. 5.** Calculated bulk formation energies $\Delta E_{\beta''}^{SS}$ of selected β" configurations with compositions $Mg_xAl_{7-x}Si_4$, $x \geq 4$ ('Si on network sites only') and $Mg_xAl_{7-x-y}Si_{4+y}$, $x \geq 4$, $y > 0$. The vertical green line and attached arrow in the figure highlights the range of configurations investigated in [9].

Fig. 5 presents the full set of configurations with formation energies below –0.28 eV/solute atom as obtained from our studies. On comparing with the results of [9] (Fig. 5 in that paper), new and old formation energies appear to generally agree well. However, two key modifications of the previous

conclusions are also noted. Firstly, some of the Mg-rich configurations excluded in the earlier work (to the right of the vertical line in Fig. 5) are evidently energetically competitive. In particular, the lowest energy $Mg_6AlSi_4$ configuration from this set is within 0.01 eV/solute atom of the minimum energy configuration, β"–$Mg_5Al_2Si_4$. Secondly, our studies highlight especially one important low energy configuration (composition $Mg_5Al_2Si_4$) where the unit cell does not obey C2/m symmetries. This result stresses the importance of explicitly allowing for precipitate compositional disorder when identifying the full set of realistic configurations. We shall discuss the information in Fig. 5 further in Sec. 5, following the interface configuration studies of Sec. 4.2, 4.3. In these studies, we shall generally assume the bulk composition $Mg_5Al_2Si_4$ for the precipitate.

Table 1 displays the structural parameters for selected low energy configurations from Fig. 5, along with the results of earlier theoretical and experimental studies of β". In Table 2, calculated formation energies, when available, have been shown. Contrasting the general interest in β", the experimental information on the phase structural parameters is surprisingly limited. Only one study [7] provides data at a sufficient precision for detailed comparison with simulations. In the case of the theoretical parameters, more results – all achieved with the aid of VASP (see Sec. 3) – are available, primarily involving β"–$Mg_5Si_6$. In both the LDA (local density approximation) and GGA based studies, occasional non-negligible differences among the calculated structural parameters for formally identical configurations are noted. These discrepancies are challenging to quantify, given the lack of detailed information on convergence tests performed. We note that our chosen precision is among the highest in the context of both PW cut-off and *k*-point density. For the formation energies in Table 2, some variation is encountered. However, this is likely in the form of a shift of the entire set of configuration energies, with little influence on relative configuration stabilities. For further comments on these issues, see Appendix B.

**Table 1**

Calculated and experimentally observed structural parameters for the β" precipitate as reported in the literature. All theoretical work refers to fully optimized bulk precipitate conventional unit cells. For the contributions from the present work, the four configurations with the lowest formation energy from Fig. 5, as well as the β"–$Mg_5Si_6$ configuration, have been included. Some computational details are discussed in the text.

| Configuration | a (Å) | b (Å) | c (Å) | β (°) |
|---|---|---|---|---|
| $Mg_5Si_6$ (presumed, exp.)[a] | 15.16±0.02 | 4.05 | 6.74±0.02 | 105.3±0.5 |
| $Mg_5Si_6$ (GGA) | 15.11 | 4.080 | 6.932 | 110.4 |
| $Mg_5Si_6$ (GGA)[b] | 15.13 | 4.05 | 6.96 | 110 |
| $Mg_5Si_6$ (GGA)[c] | 15.12 | 4.084 | 6.928 | 110.5 |
| $Mg_5Si_6$ (GGA)[d] | 15.14 | 4.05 | 6.94 | 110 |
| $Mg_5Si_6$ (LDA)[b] | 14.88 | 3.97 | 6.83 | 110 |
| $Mg_5Si_6$ (LDA)[e] | 14.95 | 3.89 | 7.00 | 110.2 |
| $Mg_5Al_2Si_4$ (GGA) | 15.32 | 4.075 | 6.778 | 105.9 |
| $Mg_5Al_2Si_4$ (GGA)[f] | 15.50 | 4.05 | 6.74 | 106 |
| $Mg_4Al_3Si_4$ (GGA) | 15.11 | 4.131 | 6.615 | 106.6 |
| $Mg_6AlSi_4$ (GGA) | 15.59 | 4.069 | 6.830 | 106.1 |
| $Mg_5Al_2Si_4$–II (GGA) | 15.39 | 4.099 | 6.692 | 106.5 |

[a][7]; [b][24]; [c][17]; [d][36]; [e][37]; [f][9]

**Table 2**

Calculated formation energies for the β" precipitate as reported in the literature. The last two columns refer to two different ways of obtaining this quantity: in the first column, $\Delta E_{\beta'', \mathrm{Bulk}}$ was

determined relative to formally isolated solute atoms in an fcc Al matrix. In the second column, these reference energies were changed to those of solute atoms in their respective bulk phases.

| Configuration | $\Delta E_{\beta''}$ (eV/solute atom) | |
|---|---|---|
| $Mg_5Si_6$ (GGA) | –0.2665 | - |
| $Mg_5Si_6$ (GGA)[a] | - | 0.0342 |
| $Mg_5Si_6$ (GGA)[b] | - | 0.0343 |
| $Mg_5Si_6$ (GGA)[c] | - | 0.0362 |
| $Mg_5Si_6$ (GGA)[d] | –0.2436 | 0.0415 |
| $Mg_5Si_6$ (LDA)[a] | - | –0.0093 |
| $Mg_5Si_6$ (LDA)[d] | –0.2270 | –0.0031 |
| $Mg_5Al_2Si_4$ (GGA) | –0.3456 | - |
| $Mg_4Al_3Si_4$ (GGA) | –0.3411 | - |
| $Mg_6AlSi_4$ (GGA) | –0.3380 | - |
| $Mg_5Al_2Si_4$–II(GGA) | –0.3309 | - |

[a][24]; [b][36]; [c][38]; [d][25]

*4.2.The β''/Al (130)$_{Al}$ interface*

*4.2.1. Overall energy variation*

Fig. 6a shows the calculated evolution in the β"–$Mg_5Al_2Si_4$/Al $(130)_{Al}$ interface supercell relative energies $\Delta E_i$ with the number of solute atoms Mg, Si contained in the precipitate. These results refer to a 'preliminary' set of interface configurations $\{i\}$, described in the next paragraph. Basic details of this approximated evaluation of relative interface configuration stabilities have been outlined in Sec. 3.1. As expected (see Sec. 2.3), the accumulated average energy change over a full cycle of configurations compares rather well with the predictions for the actual growth path. This is

directly visible in Fig. 6a from the closeness of the last configuration energy with the horizontal line. We infer that configuration energies may well be safely compared over the entire range covered in the investigations (see Appendix A for further discussion).

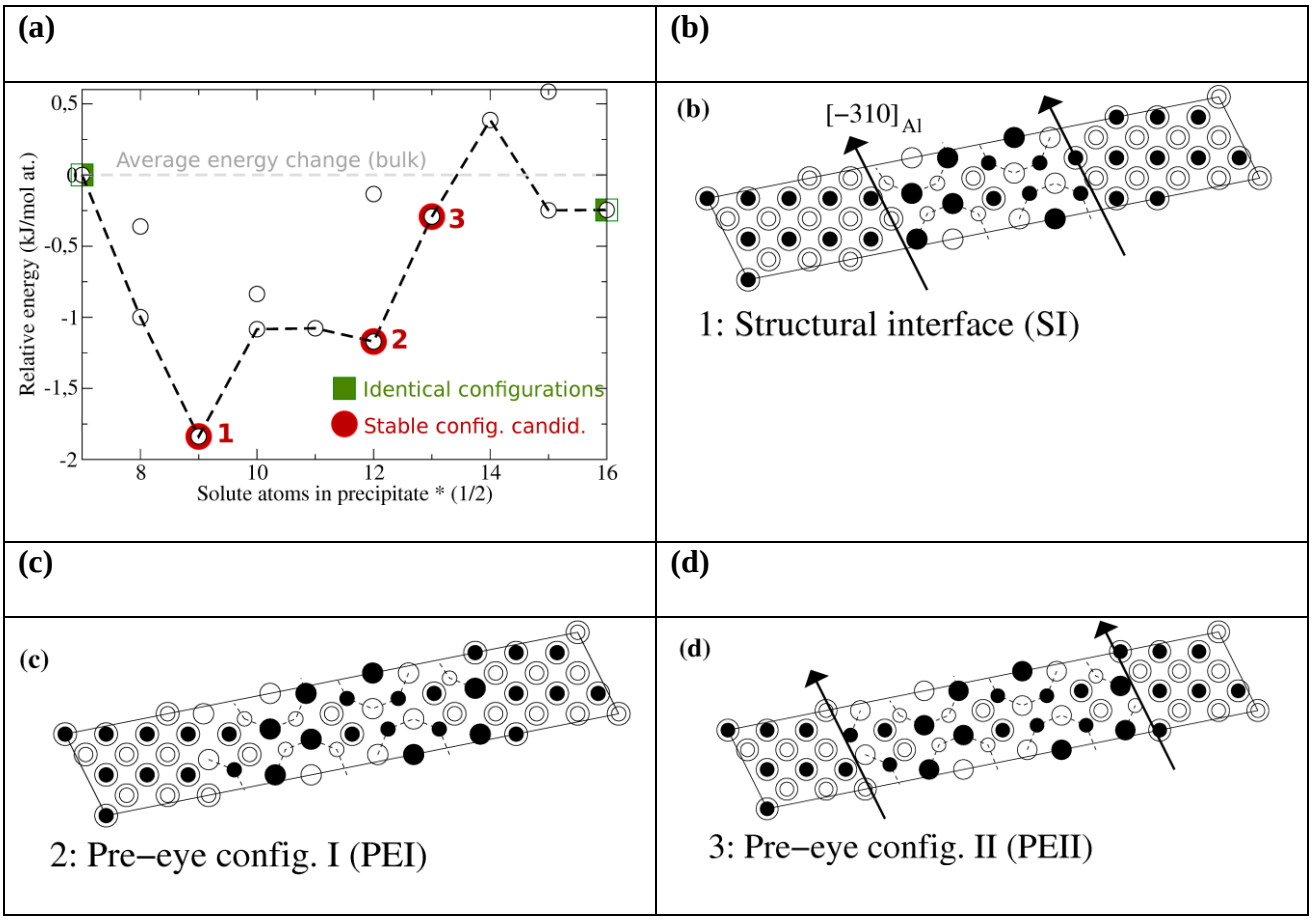


**Fig. 6.** (a) Calculated relative stabilities for a full cycle of β"–$Mg_5Al_2Si_4$/Al $(130)_{Al}$ interface configurations (preliminary suggested growth path, see text), as estimated using (3) and dividing by a factor of two. The path coupling the (logically connected) energetically most favourable configurations at each step has been highlighted with a dashed line through the data points. Three configurations with apparent local stability are labelled. (b) – (d) Schematic illustrations of the stable interface configuration candidates in (a). Atom labelling as in Fig. 1. Note that, for clarity, the added solute atoms in (c), (d) have been moved to bulk β" positions, even though all atoms in the host lattice still occupy S sites. Partly and fully constructed eye units in β" have been emphasized with thin dashed lines. The arrows, marking the approximate interface position, have been avoided

in (c), due to interface curvature.

The studies underlying Fig. 6a technically assume the complete absence of solute atom diffusion within β", even right at the interface. Precipitate extensions relative to the configuration shown in, e.g., Fig. 6b correlate with the arrows in this figure gradually moving outwards, into fcc Al. Solute atoms replace host lattice atoms only in the wake of these arrows, always occupying the sites compatible with bulk β"–$Mg_5Al_2Si_4$. Occasionally, two different sites are passed by the moving arrows roughly simultaneously. In such a case, additions of two different solute atoms is considered 'equally likely' in the proposed growth sequence, and the subsequent configuration in the sequence involves addition of both of these atoms. Obviously, this model scheme rests on a series of simplistic assumptions, to be addressed in more detail in the remainder of this text. At the same time, within the assumption of low solute atom diffusion in β", the energy variations in Fig. 6a may well be qualitatively correct. Unless otherwise noted, we shall assume below that all candidates for regions of local stability on the physical β" growth path have been highlighted by this preliminary model scheme.

Fig. 6a stresses two candidates for such regions of local stability. Following the discussion in Sec. 2.3, we search for local minima on the curve connected with the practical growth path. Two such minima are clearly visible. In the first case (global minimum), the associated configuration is the SI configuration introduced in Sec. 2.2.2. This configuration is shown schematically in Fig. 6b. However, also another (local) energy minimum is encountered in Fig. 6a, centred on the configuration displayed in Fig. 6c, but extended to potentially include the adjacent configuration in Fig. 6d. These configurations are passed roughly halfway towards completion of the next β" eye units in the supercell – explaining the labelling 'PEI', 'PEII', where PE is short for 'pre-eye'. For all other configurations examined, a solute atom can be added at an energy gain roughly equal to or

higher than the average value. Given the stability of the β" phase itself at the materials temperatures of practical interest here, the average binding energy should be a sufficient criterion for 'strong atom binding'. For this reason, the additional studies in the remainder of this section are concerned only with quantifying the level of stability of the configurations in Fig. 6b – d. When considering improvements of the preliminary growth path of Fig. 6a, we shall frequently assume that solute atom permutations relative to the bulk β"–$Mg_5Al_2Si_4$ ordering are suppressed for the entire precipitate. Whenever this constraint is imposed, we refer to the associated configuration(s) as located on a 'strict β"–$Mg_5Al_2Si_4$ growth path'.

*4.2.2. Energy variations around the β"/Al structural interface*

Turning to the β"/Al $(130)_{Al}$ SI configuration (Fig. 6b), we consider the outermost solute atoms – four per interface – forming bonds with Al atoms viewed as belonging to either precipitate or host. For each of these atoms, we examined the energy gain associated with the scenario where the SI configuration is completed through the addition of this atom exactly. This study was performed in order to ensure a significant stability of the SI configuration relative to all 'adjacent' configurations connected with smaller precipitates (earlier growth stages in the model scheme).

Likewise, we would want to verify that the SI configuration is stable against addition of more solute atoms (i.e., further growth in the model scheme). For these investigations, we calculated the supercell energy changes upon adding one solute atom that would subsequently form bonds to a precipitate atom already present in Fig. 6b. We note that the detailed considerations here need to take into account that some Al atoms are incorporated in the precipitate at this growth stage (compare e.g. Fig. 6b, d). Mg and Si additions on these β" 'Al sites' – i.e., a local departure from strict β"–$Mg_5Al_2Si_4$ growth – was examined as well, for reasons to be discussed further below.

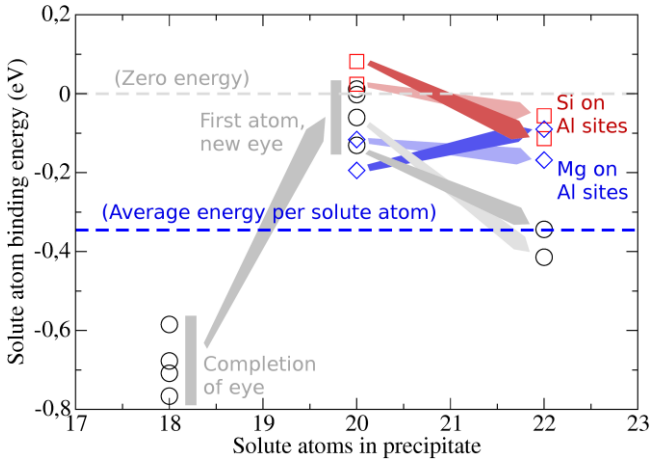


**Fig. 7.** Calculated individual solute atom binding energies in the vicinity of the SI configuration for the β"–$Mg_5Al_2Si_4$/Al $(130)_{Al}$ interface. The left arrow in the figure points to the location of the first added solute atoms to this configuration. The results suggest that this particular step on the growth path is connected with energy gains decisively lower than the average value, implying stability of the SI configuration.

The results of these studies have been included in Fig. 7. With the constraints of strict β"–$Mg_5Al_2Si_4$ growth imposed (circles in the figure), the SI configuration stability is well supported. The outermost solute atoms of this configuration bind with energies of ≈ 0.6 eV or more, well below the calculated β"–$Mg_5Al_2Si_4$ formation energy (–0.3456 eV/solute atom). By contrast, the next added solute atoms all bind weakly (0.1 – 0.15 eV/atom), or not at all. For those two added atoms that do show some level of binding, simultaneous addition (yielding 22 solute atoms in β") leads to a stable configuration, as judged from a comparison with the average energy gain. This indicates that the SI configuration stability is quite localized, with the main obstacle to further β" growth being the addition of the next *single* solute atom.

The results of adding Mg and Si to the outermost Al sites of β" have also been included (diamonds and squares, respectively) in Fig. 7. These investigations probe local transitions into other β"

compositions. One of these is the β"–$Mg_5Si_6$ configuration, obtained here when Si replaces both Al site atoms. Interestingly, this replacement is not associated with any energy gain for the single atom substitutions (and only negligible gain for simultaneous addition). The two single Si atom binding energies both reside above the zero energy value in Fig. 7. As shown in Fig. 5, the bulk β"–$Mg_5Si_6$ formation energy is clearly above that of β"–$Mg_5Al_2Si_4$. Hence, the results of Fig. 7 should likely be interpreted as stressing the complete absence of any drive for incorporating Si onto the β"–$Mg_5Al_2Si_4$ Al sites. This conclusion, already indicated in earlier studies of bulk β" [9], is in marked contrast to the conventional hypothesis [11, 27] that the more accurate β" composition is $Mg_5Si_6$.

The addition of Mg atoms onto the Al sites also holds potentially important information. The binding energy (0.19 eV) for one of these atoms is the lowest among the single solute atom additions considered here. At the same time, the value remains fairly weak compared to the average energy gain. Hence, the result is not clearly altering the conclusion of a local stability of the SI configuration. We shall return to this topic in Sec. 5.

*4.2.3. Energy variations when passing the β" eye atom*

Compared to the SI configuration stability studies in Sec. 4.2.2, examination of the PEI and PEII configurations presents some additional complexity. As discussed in Sec. 2.2.2, it is conceivable that the outermost parts of β" structurally resemble the pre–β" phase, i.e., all atoms in the vicinity of the interface may actually reside at or very near fcc Al lattice sites. This scenario is presumably most likely to occur when an eye atom is close to the interface, but still in the host – a situation encountered in both Fig. 6c, 6d. Here, it would seem necessary to compare the stability of configurations with this eye atom on S and I sites, to determine when an energy drive for a movement to the latter site appears. Another intricacy is connected with the shallow nature (see Fig. 6a) of the energy minimum comprising the PEI configuration. Given the simple growth path in

these preliminary studies, it is not entirely clear that this configuration is actually the best choice available. To examine the PEI configuration stability further, we chose to compare the energies of all configurations on strict β"–$Mg_5Al_2Si_4$ growth paths, with the same precipitate size as this configuration. Finally, a possibility of local composition modifications due to pre–β" growth is present in principle. This latter issue is largely ignored for simplicity in our studies, however, with only few deviations from strict β"–$Mg_5Al_2Si_4$ growth considered below.

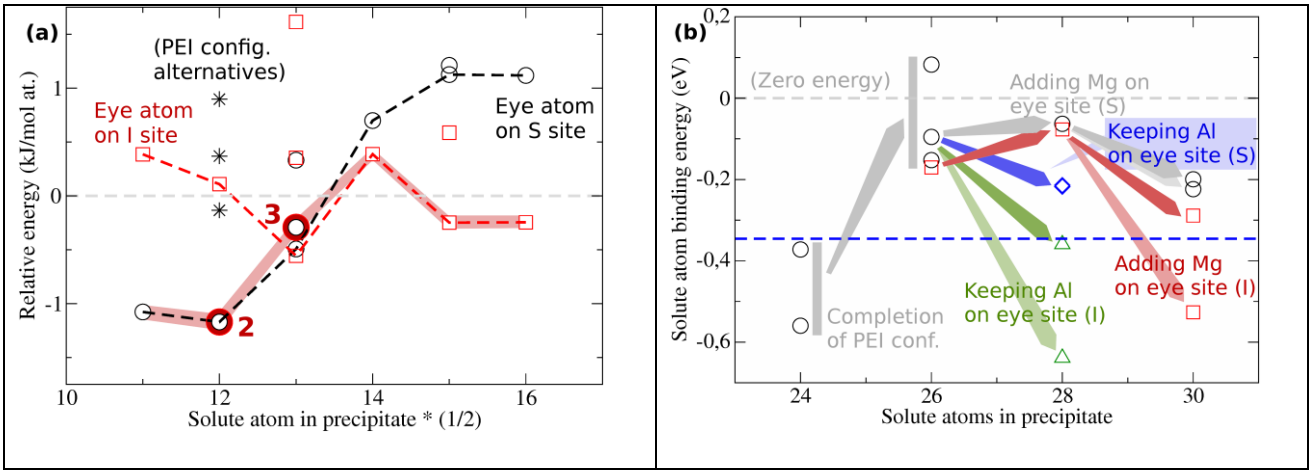


**Fig. 8.** (a) Calculated relative stabilities for β"–$Mg_5Al_2Si_4$/Al $(130)_{Al}$ interface configurations on proposed growth paths near the PEI, PEII configurations of Fig. 6c, d. The proposed path of Fig. 6a has been highlighted with a full broad line, with the position of the PEI and PEII configurations stressed. (b) Calculated individual solute atom binding energies in the vicinity of the PEI and PEII configurations. The left arrow in the figure points to the addition of the first solute atoms to the PEI configuration. The results suggest stability of the PEI configuration only, as the (adjacent) PEII configuration can be favourably extended by keeping Al on the eye site.

Fig. 8a compares selected configuration pairs around PEI and PEII with the eye atom on the S and I sites (circles and squares, respectively). The growth path of Fig. 6a (broad red line in Fig. 8a) is a mixture of these two options, with the eye atom moving to the I site as soon as it hosts an Mg atom. The calculated energies show a lack of preference for an eye atom movement to the I site up to the

point where the PEI configuration is reached (0.37 eV energy penalty). While this behaviour is expected, the energy penalty has vanished already for the adjacent PEII configuration. For all further stages of growth in Fig. 8a, I site configurations are favoured over the S site counterparts. We still stress that both the PEI and PEII configurations are reached from systems clearly defined by an eye atom preference for the S site. Hence, we regard eye atom movements as suppressed until subsequent configurations are reached. Fig. 8a also supports the PEI configuration stability over alternative configurations (stars) of the same size. We therefore conclude that investigations following the strategy of Sec. 4.2.2 can justifiably be carried out for this configuration.

As shown in Fig. 8b, we find the PEI configuration local stability to be supported by our studies. For the adjacent PEII configuration, also examined in Fig. 8b, only solute atom additions require investigation. Actually, see Fig. 8a, this configuration is slightly (0.20 kJ/mole atom) less favourable than a closely related alternative. These configurations differ by an Si–Al permutation for the outermost Si atom in Fig. 6d. More importantly, though, we note from Fig. 8b that extending the PEI configuration by addition of an Mg atom at the eye site involves an energy penalty of ≈ 0.1 eV (circle above the zero energy line). The PEII configuration stability has been judged in Fig. 6a on the basis of this Mg atom addition being the 'logical' next step in the growth sequence. However, given that the Mg replacement on the eye site is apparently generally unfavourable at this stage of growth, we may be asking ourselves if this process is avoided in practice. This in turn could have important consequences to the PEII configuration analysis.

Investigations into the above issue (Fig. 8b) support our suspicion. A calculated energy gain of more than 0.6 eV can be achieved when extending the PEII configuration by the following two-step process: firstly, (i) we add the next Mg atom to the boundary of the eye unit, as opposed to eye site, i.e., a local β"–$Mg_4Al_3Si_4$ growth mode is adopted. In addition, (ii) we move the (Al) eye atom to

the I site. As shown in Fig. 8b, both points in this single solute atom addition process are crucial, with only ≈ 0.2 eV gained if the eye atom stays on the S site. An outstanding question in our studies hence is whether the barrier to the eye atom movement is sufficiently reduced for the process to be thermally activated. We note, however, that earlier calculations on bulk β" [27] indicate a vanishing barrier for even rather Al–rich ($Mg_2Al_5Si_4$) phase compositions. Arguably, these results support the possibility of the eye atom movement being triggered in the interface evolution considerations of interest in this work. Further, as stressed earlier in this section, an inherent drive for such a movement would be presumed only when extending the precipitate *beyond* the PEII configuration. Only at this point is the I site position significantly favoured over the S site. We hence propose that, in contrast with the original conclusions of Fig. 6a, the PEII configuration is unstable.

Compared to β"–$Mg_5Al_2Si_4$, the bulk β"–$Mg_4Al_3Si_4$ configuration with Al on the eye site is found to be slightly less stable, see Sec. 4.1. Hence, the beneficial effects of circumventing Mg incorporation on the eye site are quickly diminished upon further precipitate growth. We would be cautious about concluding from the results in Fig. 8b that the presence of Mg on the eye site is ultimately entirely avoided throughout the precipitate [39]. For further discussion into the implications of the supercell results in this context, see Sec. 5.

### *4.3. The β"/Al $(–320)_{Al}$ interface*

#### *4.3.1. Overall energy variation*

Compared with the $(130)_{Al}$ interface investigation of Sec. 4.2, results for the β"/Al $(–320)_{Al}$ interface configuration relative stabilities are expected to display close similarities. This qualitative statement rests on the similar structural and chemical appearance of the bulk β" phase along the directions of the two basis vectors **a** and **c** (see Fig. 1). Fig. 9a shows the results of a preliminary investigation (following the strategy of Sec. 4.2.1) of the β"/Al interface supercell energy evolution

upon strict β"–$Mg_5Al_2Si_4$ growth. Comparing with Fig. 6a, candidates for interface configurations of local stability are obtained at the same points on the curve. Further, the associated configurations outlined in Fig. 9b – d display close similarities to the candidates of Fig. 6b – d. However, additional candidates are also encountered, connected with a comparatively stronger stability of the β"/Al $(–320)_{Al}$ SI interface configuration. On the one hand, these preliminary results would appear to justify less exhaustive studies for the $(–320)_{Al}$ interface, when focus is on the features already well analysed in Sec. 4.2. On the other hand, special attention is needed for the stable configuration candidates unique to this interface.

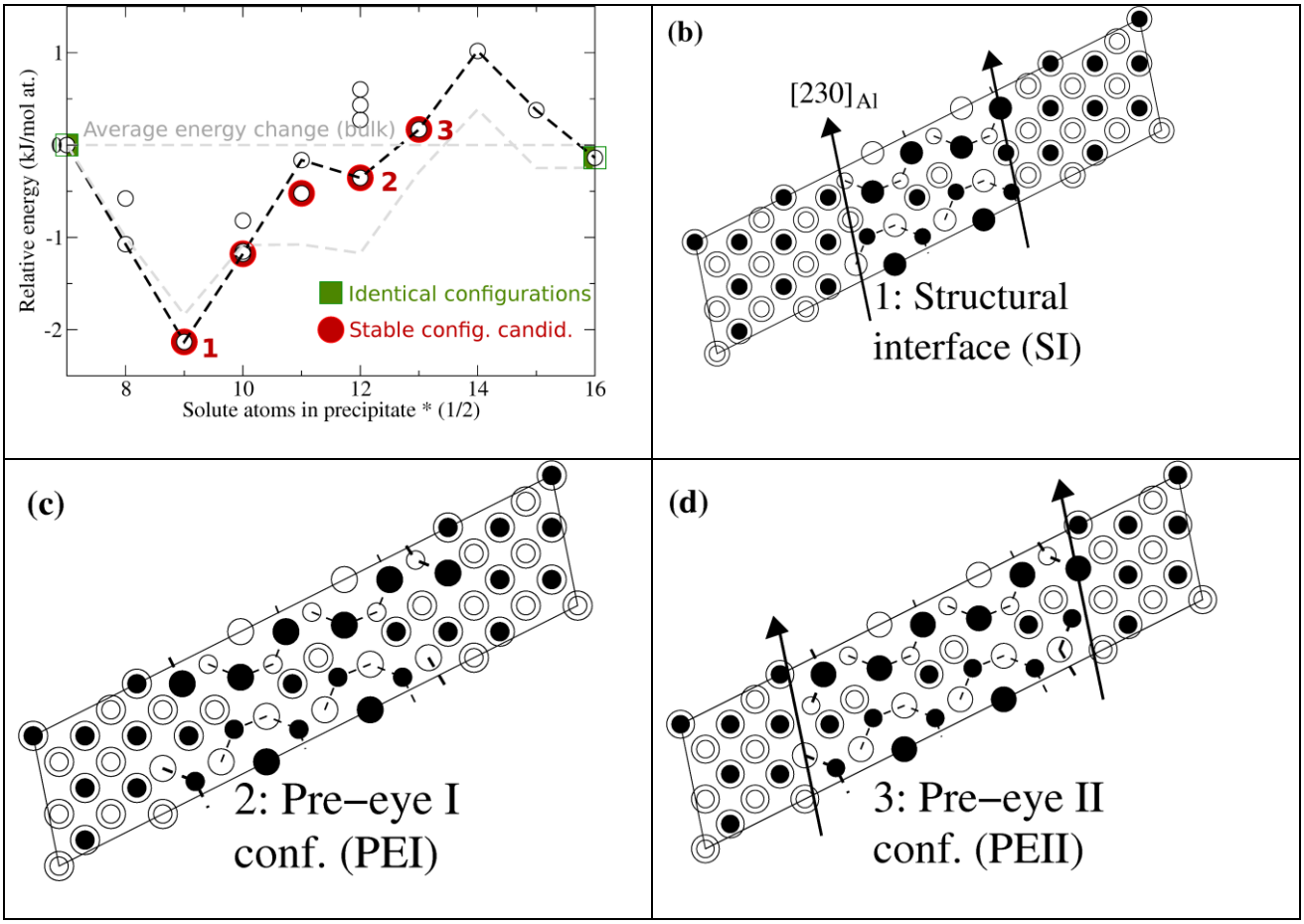


**Fig. 9.** (a) Calculated relative stabilities for a full cycle of β"–$Mg_5Al_2Si_4$/Al $(–320)_{Al}$ interface configurations (preliminary suggested growth path, see text), as estimated using (3) and dividing by a factor of two. Corresponding results for the β"/Al $(130)_{Al}$ (**cb**) interface (Fig. 6a) have been included for comparison. Five configurations with apparent local stability are highlighted; three of

them labelled. (b) – (d) Schematic illustrations of the interface configurations labelled in (a). The arrows highlighting the interface position have been avoided in (c) due to interface curvature. See Fig. 6 for details on the nomenclature.

*4.3.2. Energy variations around the stable interface configuration candidates*

The calculated solute atom binding energies in the vicinity of the SI configuration (Fig. 9b) for the β"/Al **ab** interface have been shown in Fig. 10. Qualitatively, no differences are present compared with the corresponding **cb** interface results (Fig. 7), and even a quantitative comparison does not suggest any variations worthy of note. Once again, the SI configuration is decisively stable in the proposed precipitate growth scheme. Incorporation of Mg on the Al sites represent the most favourable single atom additions, but still with these binding energies being markedly weaker (≈ 50%) than the β"–$Mg_5Al_2Si_4$ formation energy. Solute atom pair additions are discussed at the end of this section.

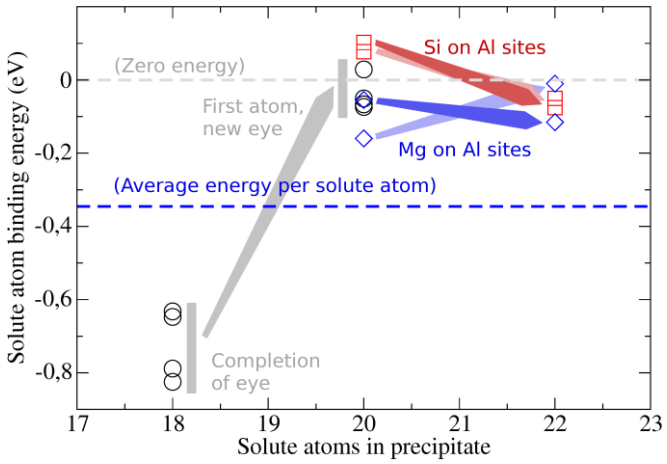


**Fig. 10.** Calculated individual solute atom binding energies in the vicinity of the SI configuration for the β"–$Mg_5Al_2Si_4$/Al $(–320)_{Al}$ interface. Compare with Fig. 7.

Also the energy variations around the PEI and PEII configurations for the β"/Al **ab** interface show

clear resemblance to the corresponding conclusions (Fig. 8b) for the **cb** interface. In addition to the results included in Fig. 11, our studies here probed the main features of the discussion in Sec. 4.2.3. Firstly, we ensured that configurations with the eye atom on the I site are never clearly favoured over their S site counterparts in energy, until the point when the PEII configuration has been passed. Secondly, the PEI configuration stability relative to alternative candidate configurations of the same size was supported, see Fig. 9a. And finally, when passing the PEII configuration, we compared – for configurations with the eye atom at the I site – the energy gain upon incorporation of Mg on the eye site vs. the boundary of the eye unit. The results of this study, shown in Fig. 11, confirmed our expectations. Not only is the latter growth path clearly favoured over the former – it is also sufficiently favourable to render the PEII configuration unstable. As in Sec. 4.2.3, this conclusion rests on an expectation of a low activation energy for the eye atom movement to the I site at this stage of growth.

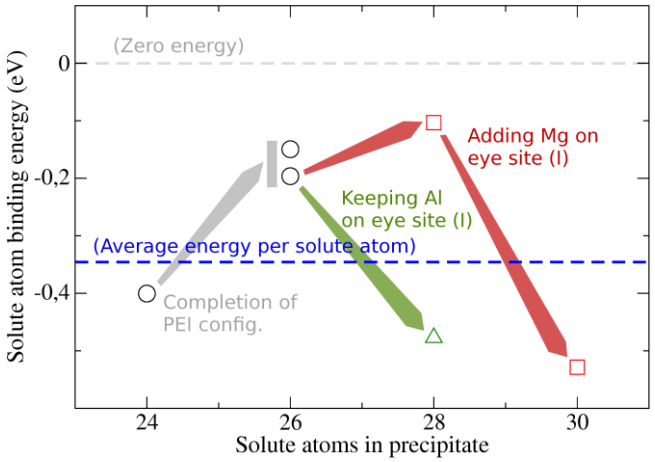


**Fig. 11.** Calculated individual solute atom binding energies in the vicinity of the PEI and PEII configurations for the β"–$Mg_5Al_2Si_4$/Al $(–320)_{Al}$ interface. Compared to Fig. 8b, highly similar trends in the binding energies are noted, with only the PEI configuration displaying stability.

To address the stable interface configuration candidates of Fig. 9a unique to the β"/Al **ab** interface,

we examined selected atom pair additions, on strict β"–$Mg_5Al_2Si_4$ growth paths, to the SI configuration. In these studies, Mg-Si enriched SI configurations involving the Si atom not binding on its own in Fig. 10 were ignored for simplicity. The results obtained did not affect the conclusions of Fig. 9a. Judged from the PEI configuration stability studies already discussed, alternative energetically favourable β"–$Mg_5Al_2Si_4$ growth paths seem unlikely. In conclusion, no new stable interface configuration candidates were revealed here.

## *5. Discussion*

### *5.1. Compositional disorder in β"*

When discussing the bulk β" configuration stabilities in Sec. 4.1, we examined the results of Fig. 5 in the conventional manner. The general implicit assumption in this analysis is the absence of significant diffusion constraints in the precipitate. The only direct limitation introduced is that all configurations addressed be isostructural to β". At the point where the formation energy attains its minimum, the solute atoms (along with Al) will fully occupy their respective preferred sites in this set-up. Technically, our choice of reference energies in (4) may induce some bias to the relative configuration stabilities. By comparison, the issue of precipitate compositional disorder is typically entirely postponed until subsequent discussions.

When comparing these considerations with the interface configuration studies of Sec. 4.2, 4.3, a potentially altered picture emerges. Firstly, the SI configuration stability studies have indicated the probability of Mg replacement (as opposed to the usually proposed Si replacement) of one or both of the β"–$Mg_5Al_2Si_4$ Al atoms. In other words, a theoretical drive for stabilizing one or more β"–$Mg_{5+x}Al_{2-x}Si_4$ configurations with $x > 0$ has been proposed here. Secondly, the PEI configuration stability studies have indicated a reduced occupancy of Mg on the eye site (in favour of Al), due to growth obstacles. Here, the potential stabilization of a β"–$Mg_{5+x}Al_{2-x}Si_4$ configuration with $x < 0$ is

highlighted. It is evident that a combination of these two effects may roughly preserve the $Mg_5Al_2Si_4$ composition of β" suggested in [9], but with a non-negligible level of compositional disorder introduced. Such a conclusion is not simply identical to a proposed mixing of the lowest energy configurations in the analysis underlying Fig. 5. The degree to which that mixing would be rendered probable is connected with stabilizing effects due to increased configuration entropy. By contrast, the conclusions from our interface configuration studies is linked to an assumption of diffusion constraints in β". As such, our proposed mechanism potentially enhances the level of precipitate compositional disorder.

At the present stage, the issue raised above is inherently complex, given that it involves the influence of parameters – namely, atom diffusion in β" – not closely examined in the literature (see Sec. 2.2.1). In this context, the investigations of the present work should be viewed also as a motivation for further studies into the details of β" growth. In particular, the bulk of our studies have assumed that the $Mg_5Al_2Si_4$ composition is only locally altered. Given the level of disorder revealed when incorporating such local composition modifications, we cannot justifiably exclude that the full degree of theoretically proposed disorder is even higher. Accompanying more detailed considerations following our chosen strategy, dynamical studies into the same issues – if sufficiently accurate – should be highly encouraged.

*5.2. Examination of alternative interface configurations*

Both the β"/Al $(130)_{Al}$ and $(–320)_{Al}$ interface configuration stability investigations suggest the presence of an additional candidate configuration, PEI, as an alternative to the SI configuration highlighted in [17] (for β"–$Mg_5Si_6$ studies) and [18]. For both interfaces, the SI configuration is associated with a considerably lower interface energy (see Table 3). Adding to these considerations the clearly changed structure of the PEI configuration, a physical presence of two locally stable

configurations on the β" growth path may have considerable influence on precipitate evolution. For comparison with earlier work, Table 3 also includes the β"–$Mg_5Si_6$ SI interface configuration energies from [17].

**Table 3**

Calculated interface energies for the locally stable β"/Al interface configurations reported in the literature. The interface energies for the SI configurations are obtained using standard procedures, see, e.g., [17], while the PEI energies are obtained from Fig. 6a, 9a.

| Precipitate, interface | Configuration | Interface energy (kJ/mol at.) |
|---|---|---|
| $Mg_5Al_2Si_4$, $(130)_{Al}$ | SI (Fig. 6b) | 1.66 |
| $Mg_5Al_2Si_4$, $(130)_{Al}$ | PEI (Fig. 6c) | 2.33 |
| $Mg_5Al_2Si_4$, $(–320)_{Al}$ | SI (Fig. 9b) | 1.20 |
| $Mg_5Al_2Si_4$, $(–320)_{Al}$ | PEI (Fig. 9c) | 3.08 |
| $Mg_5Si_6$, $(130)_{Al}$[a] | SI | 1.06 |
| $Mg_5Si_6$, $(–320)_{Al}$[a] | SI | 1.27 |

[a][17]

Following the detailed studies of Sec. 4.2.3, 4.3.2, the PEII configuration was identified as the least favourable configuration on the proposed β" growth path. This conclusion is valid to both interfaces. As stressed previously, the PEI and PEII configurations are adjacent on this path. Hence, the stability of the PEI configuration must be considered strongly dependent on the frequency of processes involving simultaneous addition of at least two solute atoms locally. For the β"/Al $(130)_{Al}$ interface, this consideration also applies to the SI configuration (see Fig. 7), however. Further, experimental observation supports the existence of at least one stable interface configuration. We

infer that the proposed PEI configuration local stability is likely real, unless our theoretical growth paths should strongly deviate from the physical ones.

The SI and PEI interface configurations differ solely by solute atoms occupying S sites in fcc Al. These configurations are not easily distinguishable when only interatomic distances are used as the tool for identifying the precipitate interface. The greatest exception, according to the supercell studies, occurs for the $(-320)_{Al}$ interface. Here, the outermost Si atom for the PEI configuration (Fig. 9c) moves non-negligibly closer to the line connecting the two adjacent Mg atoms. Compared to the SI configuration, this movement is accompanied by changes in certain Si–X interatomic distances by ≈ 0.3 Å – an effect that may be noticeable in experimental TEM images.

*5.3. Model limitations and improvements*

The supercell approach used in this work represents a presently necessary, though evidently highly simplifying method for probing the β"/Al interface evolution characteristics (see, e.g., [16]). A series of fundamental modelling assumptions may be addressed in the context of ensuring reliability in the theoretical conclusions. The influence of supercell size, in the direction perpendicular to the interface, was examined in Appendix A, and found to be weak. Along the β" main growth axis (direction out of the plane in, e.g., Fig. 3) the cell dimension is kept at ≈ 4 Å. In practice, this implies that the interface evolves by addition of *columns* of solute atoms with the same atom separation, as opposed to isolated atoms. We do not dispute the presence of potentially important limitations of the supercell description in this context. As an example, single vs. collective eye atom movements may be an issue to consider further by use of larger cells. However, we also stress that the use of such cells naturally introduces the need for a more refined growth model.

For the zero temperature investigations of this work, the potentially largest source of errors remains the probing of the growth path. Future studies may benefit from adopting a more exhaustive approach, with interface configurations involving larger curvature, as well as stronger local deviations from an expected bulk β" composition. Such studies could presumably use as a safe starting point the SI configuration. There must seem little doubt (see Fig. 6a and 9a) that this configuration is located on the physical growth path. We note that, even when allowing for large levels of compositional disorder, it would seem unlikely that transitions into post–β" phases are probed. Given the lower degree of coherency for those precipitates, such transitions should be associated with triggering larger structural deviations from the underlying fcc Al host lattice.

Our studies have ignored finite temperature corrections throughout. In the literature, such corrections have been discussed up to now at the atomistic level only for the bulk β" phase [36, 38]. Other theoretical work [40] has involved an attempted determination of the interfacial energy σ from experimental data. Here, a value of 45 mJ/m² was reported. This result is more than a factor two below purely DFT based values [17, 18] for the SI configuration, with the calculations of [18] employing the precision of the present work. When turning to the bulk formation energy, we note a similar discrepancy to the results of [40]. Since no such strong influences of temperature have been suggested in other work [36, 38], we would be cautious to challenge our interface configuration conclusions on the above basis. Generally, however, it is expected that the diffuse nature of the interface configuration should increase with temperature, inducing an interfacial energy decrease, see, e.g., [41]. The outstanding question, at this stage, is the extent to which the determination of locally stable interface configurations and the effects of temperature can be decoupled in the analysis. This is a pressing topic of future work.

Finally, the presence of interface configurations incompatible with a preserved precipitate

stoichiometry presents a basic challenge on its own. As stressed in Sec. 1, no framework is currently available for determining the interfacial energy in these situations. Both the present work and the results of [19] highlight candidate configurations from this more challenging category, and hence should strongly motivate investigations into a more generalized interfacial energy analysis.

## 6. Conclusions

We have examined β"/Al interface configuration relative stabilities for the experimentally reported coherent interfaces, $(130)_{Al}$ and $(\bar{3}20)_{Al}$, using DFT. While our studies have employed a conventional supercell description, we have relaxed the usual constraint of a preserved precipitate stoichiometry in the cell. Assuming negligible solute atom diffusion at the precipitate boundary and interior in the calculations, we have outlined the configuration energy variations on layer-by-layer growth paths covering the full periodic range of β" evolution. Our assumption is not simply a mere simplification – it also connects with the lack of knowledge on the physical system behaviour. The interface configuration studies highlight local growth obstacles, the importance of which is intimately connected to the outstanding diffusion issue. We stress the potential presence of appreciable amounts of Al (Mg) on the eye site (Al sites) in β"–$Mg_5Al_2Si_4$ – the energetically most favourable bulk configuration reported [9]. Our own bulk β" studies support a competitive nature of both locally Al-rich and Mg-rich configurations. Further, β"–$Mg_5Si_6$ – often mentioned as the most likely precipitate configuration in the literature – is clearly excluded on the basis of our interface configuration studies. The Si atoms are neither replacing Al at an energy gain near the interface, nor in the bulk. For both β"/Al interfaces examined, our studies highlight the presence of a locally stable alternative to the structural interface configuration highlighted in [17, 18]. This new candidate configuration has markedly different structure and interface energy, and hence may significantly influence β" growth characteristics.

**Acknowledgements**

This work has been financially supported by the Research Council of Norway via the MultiModAl project (project no. 205353). Simulations were performed through access to the NOTUR facilities. The author would like to thank Dr. D. R. Bowler, University College London and Dr. A. P. Horsfield, Imperial College London, for useful discussions relating to Sec. 5.

## Appendix A. Cell size convergence studies

A series of studies have been performed in order to test that the supercells used for the interface configuration stability studies of Sec. 4.2, 4.3 are sufficiently large to avoid bias in any configuration energies. The 55 atom cells used in the calculations on β"/Al **cb** interface configurations were extended by adding either (i) a β" primitive unit cell or (ii) a 'corresponding' fcc Al supercell. The latter was constructed from Fig. 1 by moving the eye atom to the fcc site and substituting Al for the Mg and Si atoms. Configurations in the vicinity of the two stable interface configuration candidates, SI (Fig. 7) and PEI (Fig. 8b), were then examined and compared with the results of the original 55 atom cell studies. To reduce computational costs in this procedure, a PW cut-off of 170 eV and a (2, 11, 7) *k*-point grid was employed throughout. This included a set of new 55 atom cell based energies that were compared in turn to the results of Sec. 4.2. For simplicity, only **cb** interface configurations were examined in this manner.

The calculated influence of cell size on relative configuration stabilities, as obtained on the basis of the above studies, is shown in Fig. A1. Generally, the change of precision is found to be the key source of changes to the binding energies, with modifications approaching 0.1 eV. This issue is discussed further in Appendix B. By comparison, changing the supercell size has insufficient influence on the binding energies for the ordering to be affected. Here, energy modifications are everywhere well within 0.1 eV. These results strongly suggest that the 55 atom cells used

throughout our work are sufficiently large for the intended purpose.

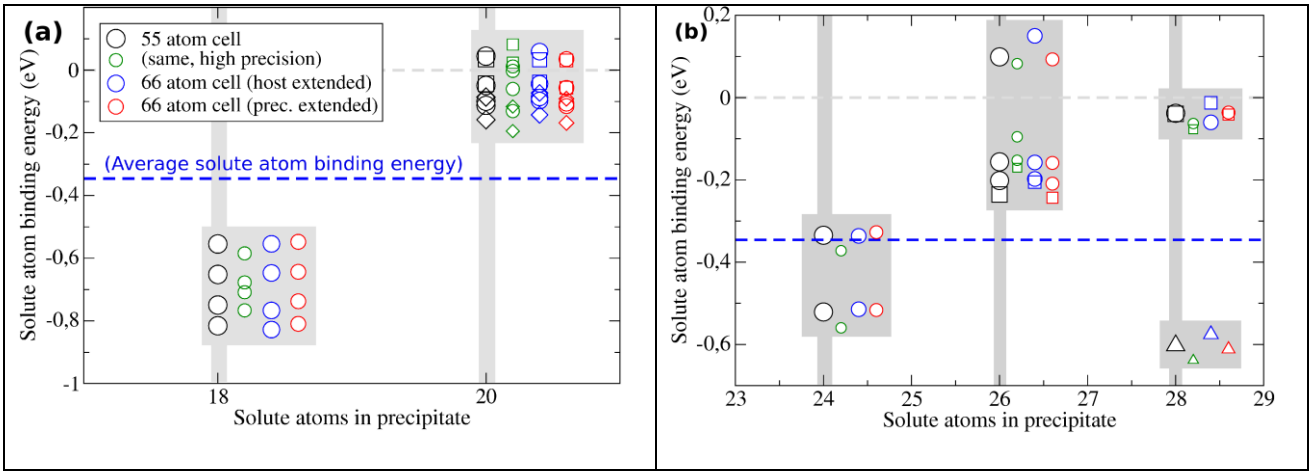


**Fig. A1.** Atom binding energies as a function of precision as well as precipitate and host lattice size, for (a) the SI and (b) the PEI β"–$Mg_5Al_2Si_4$/Al $(130)_{Al}$ interface configurations. For details on the labelling (circles vs. squares, diamonds and triangles), see Figs. 7, 8b.

## Appendix B. Precision convergence studies

When comparing the calculated β" structural parameters and formation energies from the literature in Sec. 4.1, we noted a weak, but non-negligible level of discrepancies among the output data for formally identical configurations. The source of these variations is difficult to quantify, given lack of sufficient information on the convergence tests performed in the underlying studies. Further, in Appendix A, we found indications that precision, rather than cell size, may be the main source of errors to the interface configuration relative stabilities within our chosen set-up. These two considerations both serve as motivation for outlining, in sufficient detail, convergence test results for selected configurations.

To examine the energy convergence with PW cut-off for the broad range of interface configurations of, e.g., Fig. 6a, we calculated the variation in the energies of three representative systems for cut-offs in the range 150 – 275 eV. These systems were (i) bulk β"–$Mg_5Al_2Si_4$, (ii) bulk fcc Al, and (iii)

a substitutional Mg-Si pair in fcc Al. The first two systems couple to the SI configuration, with the third system mimicking the influence of precipitate growth. In all cases, cells with the size of a β" primitive unit cell (Fig. 1) were employed, in order to eliminate the influence of different *k*-point grids. Throughout the studies, a (22, 12, 14) *k*-mesh was used. Our reason for selecting a solute atom pair geometry over single solute atom cells is the observation that Mg and Si are typically nearest neighbours in β". Technically, our investigation probes the errors from both interface configuration studies simultaneously.

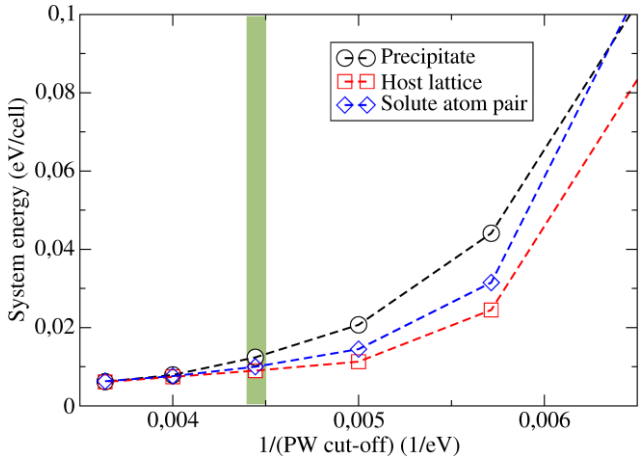


**Fig. B1.** Selected system energies as a function of PW cut-off value. All curves have been translated for zero error to be obtained at full convergence ($x = 0$). The dashed lines are guides to the eye. The horizontal line denotes the chosen cut-off value used in the bulk of this work (225 eV).

Fig. B1 displays the results of these investigations. For clarity, we estimated the fully converged energies for each system by polynomial fitting, using these values as a common zero in the output. Evidently, the convergence behaviours of the different systems are not entirely identical. However, for PW cut-off values above our choice of 225 eV (horizontal line in the figure), these effects are decisively small. Remaining corrections for the energies of interface configurations at opposite ends of the full range investigated in, e.g., Fig. 6a are unlikely to exceed 0.03 kJ/mole atom – the

accumulated correction from 4 solute atom pair additions. This value is negligible compared to the general variations in Fig. 6a. Suggested errors due to the choice of *k*-point grid (calculations performed for β" only) are roughly a factor ten smaller. Finally, the energy variation with PW cut-off for different bulk β" configurations was examined for the two energetically most favourable configurations with composition $Mg_5Al_2Si_4$. Very similar trends were observed in this case, indicating that also weak local precipitate composition fluctuations are well described. We conclude that remaining sources of errors within the studies relating to (3) are essentially negligible at our chosen level of precision. Structural parameter investigations yielded the same conclusion.

**References**

[1] C. D. Marioara, S. J. Andersen, H. W. Zandbergen, and R. Holmestad, Metal. Mater. Trans. A **36A**, 691 (2005).

[2] S. Gulbrandsen-Dahl, C. D. Marioara, K. O. Pedersen, and K. Marthinsen, Mater. Sci. Forum **706–709**, 283 (2012).

[3] S. Pogatscher, H. Antrekowitsch, H. Leitner, A. S. Sologubenko, and P. J. Uggowitzer, Scripta Mater. **68**, 158 (2013).

[4] J. Banhart, M. D. H. Lay, C. S. T. Chang, and A. J. Hill, Phys. Rev. B. **83**, 014101 (2011).

[5] G. A. Edwards, K. Stiller, G. L. Dunlop, Appl. Surf. Sci. **76/77**, 219 (1994).

[6] C. D. Marioara, S. J. Andersen, J. Jansen, and H. W. Zandbergen, Acta Mater. **51**, 789 (2003).

[7] H. W. Zandbergen, S. J. Andersen and J. Jansen, Science **277**, 1221 (1997).

[8] S. J. Andersen, H. W. Zandbergen, J. Jansen, C. Træholt, U. Tundal, and O. Reiso, Acta Mater. **46**, 3283 (1998).

[9] H. S. Hasting, A. G. Frøseth, S. J. Andersen, R. Vissers, J. C. Walmsley, C. D. Marioara, F. Danoix, W. Lefebvre, and R. Holmestad, J. Appl. Phys. **106**, 123527 (2009).

[10] H. I. Aaronson, M. Enomoto, and J. K. Lee in *"Mechanisms of diffusional phase*

*transformations in metals and alloys"* p. 438. Boca Raton, FL: CRC Press (2010).

[11] J. H. Chen, E. Costan, M. A. van Huis, Q. Xu, and H. W. Zandbergen, Science **312**, 416 (2006).

[12] V. Vaithyanathan, C. Wolverton, and L. Q. Chen, Phys. Rev. Lett. **88**, 125503 (2002).

[13] O. R. Myhr, Ø. Grong, H. G. Fjær, and C. D. Marioara, Acta Mater **52**, 4997 (2004).

[14] A. Bahrami, A. Miroux, and J. Sietsma, Metal. Mater. Trans. A **43A**, 4445 (2012).

[15] J. Allison, M. Li, C. Wolverton, and X. Su, JOM, **58** 28 (2006).

[16] Y. Mishin, M. Asta and J. Li, Acta Mater. **58**, 1117 (2010).

[17] Y. Wang, Z.-K. Liu, L.-Q. Chen and C. Wolverton, Acta Mater. **55**, 5934 (2007).

[18] F. J. H. Ehlers and R. Holmestad, Comp. Mater. Sci. **72**, 146 (2013).

[19] L. Bourgeois, C. Dwyer, M. Weyland, J.-F. Nie, and B. C. Muddle, Acta Mater. **59**, 7043 (2011).

[20] R. Bjørge, C. Dwyer, M. Weyland, P. N. H. Nakashima, C. D. Marioara, S. J. Andersen, J. Etheridge, and R. Holmestad, Acta Mater. **60**, 3239 (2012).

[21] Note that Fig. 1 shows the β" primitive unit cell, with the conventional (monoclinic) unit cell having twice the size along $[230]_{Al}$.

[22] G. Sha, H. Möller, W. E. Stumpf, J. H. Xia, G. Govender, and S. P. Ringer, Acta Mater. **60**, 692 (2011).

[23] Both of these studies strictly speaking involved Al–Mg–Si–Cu alloy systems, with low Cu amounts reported in the β" precipitates. It cannot be excluded that Cu has a non-negligible effect on the Mg/Si ratio.

[24] C. Ravi and C. Wolverton, Acta Mater. **52**, 4213 (2004).

[25] M. A. van Huis, J. H. Chen, H. W. Zandbergen, and M. H. F. Sluiter, Acta Mater. **54**, 2945 (2006).

[26] C. D. Marioara, S. J. Andersen, J. Jansen, and H. W. Zandbergen, Acta Mater. **49**, 321 (2001).

[27] M. A. van Huis, M. H. F. Sluiter, J. H. Chen, and H. W. Zandbergen, Phys. Rev. B **76**, 174113

(2007).

[28] K. Teichmann, C. D. Marioara, S. J. Andersen, and K. Marthinsen, Mater. Char. **75**, 1 (2013).

[29] Note that we extend the result of (2) here, assuming that no *particular* interface configuration energy along the growth path is comparatively strongly affected by modelling constraints. Within the chosen theoretical framework, this in turn implies that ignoring effects related to supercell size should always be safe. For details on investigations made in this context, see Appendix A.

[30] P. Hohenberg and W. Kohn, Phys. Rev. **136**, B864 (1964).

[31] W. Kohn and L. J. Sham, Phys. Rev. **140**, A1133 (1965).

[32] D. Vanderbilt, Phys. Rev. B **32**, 8412 (1985).

[33] G. Kresse and J. Hafner, Phys. Rev. B **47**, R558 (1993).

[34] G. Kresse and J. Furthmüller, Comput. Mater. Sci. **6**, 15 (1996).

[35] J. P. Perdew, J. A. Chevary, S. H. Vosko, K. A. Jackson, M. R. Pederson, D. J. Singh, and C. Fiolhais, Phys. Rev. B **46**, 6671 (1992).

[36] D. Zhao, L. Zhou, Y. Kong, A. Wang, J. Wang, Y. Peng, Y. Du, Y. Ouyang, and W. Zhang, J. Mater. Sci. **46**, 7839 (2011).

[37] R. Yu, J. Zhu, and H.Q. Ye, Comp. Phys. Commun. **181**, 671 (2010).

[38] H. Zhang, Y. Wang, S. L. Shang, C. Ravi, C. Wolverton, L. Q. Chen, and Z. K. Liu, Calphad **34**, 20 (2010).

[39] For the same reason, we would be cautious about investigating in detail the post-PEII configuration revealed by the studies in Fig. 8b. This configuration may actually be locally stable if the Mg atom stays away from the eye site. But if the Al atoms here are gradually replaced upon further precipitate growth, that stability may vanish.

[40] A. A. Vasilyev, A. S. Gruzdev, and N. L. Kuz'min, Phys. Sol. Stat. **53**, 1902 (2011).

[41] B. Sonderegger and E. Kozeschnik, Metal. Mater. Trans A **41A**, 3262 (2010).